Hydrological response of a dryland ephemeral river to southern African climatic variability during the last millennium

Benito, G.[1*], Thorndycraft, V.R.[2], Rico, M.T.[3], Sánchez-Moya, Y.[4], Sopeña, A.[4], Botero, B.A.[5], Machado, M.J.[1], Pérez-González, A.[6]

*Corresponding author:

Gerardo Benito, Institute of Natural Resources, CSIC, Serrano 115bis, 28006 Madrid, Spain. Telephone: +34 917452500; Fax: + 34 5640800; e-mail: benito@ccma.csic.es

Number of words: 8810
Tables: 2
Figures: 6

Madrid, Januray 7, 2011.

Dear Derek,

I have changed the reported format for the radiocarbon dating, to meet the guidelines of the journal. It took me a little bit of time because our radiocarbon lab reported the calibrated dates as AD years +/- error, and I had to run the calib software and re-phrase several setences of the manuscript accordingly. I have finally decided to report the dates as conventional 14C yr BP, with indication of the calibrated AD range age. I have changed the tables 1 and 3, and the figures 2 and 3, accordingly.
I believe that the manuscript is now ready for publication.

Very best wishes,

Gerardo Benito

Hydrological response of a dryland ephemeral river to southern African climatic variability during the last millennium

Benito, G.[1], Thorndycraft, V.R.[2], Rico, M.T.[3], Sánchez-Moya, Y.[4], Sopeña, A.[4], Botero, B.A.[5], Machado, M.J.[1], Pérez-González, A.[6]

(1) Institute of Natural Resources, CSIC, Serrano 115bis, 28006 Madrid, Spain

(2) Department of Geography, Royal Holloway University of London, Egham, Surrey TW20 0EX, UK

(3) Pyrenean Institute of Ecology, CSIC, Apdo. 202, 50080 Zaragoza, Spain

(4) Institute of Geosciences, CSIC-Universidad Complutense, 28040, Madrid, Spain

(5) Departamento de Ingeniería Civil, Universidad Nacional de Colombia, sede Manizales, Manizales, Colombia

(6) CENIEH -National Research Centre on Human Evolution, Burgos, Spain.

Abstract:

A long-term flood record from the Buffels River, the largest ephemeral river of NW South Africa (9250 km^2), was reconstructed based on interpretation of palaeoflood, documentary and instrumental rainfall data. Palaeoflood data were obtained at three study reaches, with preserved sedimentary evidence indicating at least 25 large floods during the last 700 years. Geochronological control for the palaeoflood record was provided by radiocarbon and optically stimulated luminescence (OSL) dating. Annual resolution was obtained since the 19th century using the overlapping documentary and instrumental records. Large floods coincided in the past within three main hydroclimatic settings: (1) periods of regular large flood occurrence (1 large flood/~30 yr) under wetter and cooler prevailing climatic conditions (AD 1600-1800), (2) decreasing occurrence of large floods (1 large flood/~100 yr) during warmer conditions (e.g., AD 1425-1600 and after 1925), and (3) periods of high frequency of large floods (~4-5 large

floods in 20-30 yr) coinciding with wetter conditions of decadal duration, namely at AD 1390-1425, 1800-1825 and 1915-1925. These decadal-scale periods of the highest flood frequency seem to correspond in time with changes in atmospheric circulation patterns, as inferred when comparing their onset and distribution with temperature proxies in southern Africa.

Key words: Palaeofloods; palaeohydrology; palaeoclimate; Buffels River, southern Africa.

1. Introduction

According to the latest IPCC report, hydrological response to global warming is one of the major uncertainties of future climate predictions (Trenberth et al., 2007). This is especially so for dryland regions, characterised by ephemeral streams (Tooth, 2000), where there is added uncertainty due to: a) a lack of monitoring station networks and hence instrumental records; and b) the spatial and temporal variability of ephemeral river flow, meaning that even for gauged ephemeral streams there are likely to be fewer observed floods than for their perennial counterparts (Schick, 1988). This is a critical issue in many arid and semi-arid environments, where quantitative estimates of the effects of climatic change on hydrology are essential for both water resource management (Morin et al., 2009; Benito et al., 2010) and flood risk planning (Milly et al., 2002).

One such dryland region particularly susceptible to changes in climate is the winter rainfall zone (WRZ) of southern Africa (MacKellar et al., 2007). The region is predicted to witness an increase in temperature of 3-4°C (after multi-model data set forced in A1B scenario in Christensen et al., 2007) and a decrease in annual runoff of 10-20% by 2041-2060, relative to the period 1900-1970 (Milly et al., 2005). This is expected to impact heavily on the natural environment over the next 100 years (Midgley et al., 2005, Midgley and Thuiller, 2007). Chase and Meadows (2007) reviewed the response of the WRZ to long term past climatic changes during the late Quaternary, indicating an expansion of the WRZ during the period 32-17 ka of the last glacial and similar expansions during cold periods of the Holocene (Tyson, 1999).

With regards the late Holocene, hydrological response to climatic variability of the last millennium can be considered of particular importance for understanding recent and future environmental change in the region. This period was characterized by Little Ice Age cooling between AD 1300-1800 (Tyson and Lindesay, 1992; Tyson et al., 2000), with the lowest temperatures coinciding with the Late Maunder (1675-1715) solar minima, according to the late Holocene record from an aragonitic stalagmite taken from Cold Air Cave in the Makapansgat Valley in north eastern South Africa (Holmgren et al., 1999, 2003; Tyson et al., 2000).

How these regional temperature variations affected the hydrology of ephemeral rivers is of interest to help understand the dynamics of hydrological response to shifts in the WRZ. This is of particular importance for the Namaqualand region of the WRZ as this is one of only two global biodiversity hotspots located in a dryland environment (Desmet, 2007) and such information would provide an environmental context for the historical socio-economic development of the region (Hoffmann and Rohde, 2007). Indeed, identifying the relative impacts of climate and land use change is a major challenge in this environmentally sensitive region (Hoffmann and Rohde, 2007; Midgley and Thuiller, 2007). The derivation of long-term flood records from sedimentological evidence (palaeoflood records) and documentary accounts can provide the basis for investigating flood response to climatic variability during the last millennium and water regime trends within these ungauged river basins.

Palaeoflood studies across many regions with diverse hydrological regimes have demonstrated their applicability in deciphering long-term hydrological response to climate variability (e.g., Knox, 2000; Redmond et al., 2002). The aim of palaeoflood hydrology is not necessarily to provide analogues of future flood-climate episodes but rather to analyse flood response to past changes in atmospheric circulation (Hirschboeck, 1988; Ely et al., 1993; Thorndycraft and Benito 2006; Benito et al., 2008). To date, palaeoflood studies in southern Africa have focused on the summer rainfall zone (SRZ), for example: Crocodile River in NW Pretoria (Smith and Zawada, 1990); Umgeni River in Natal, (Smith 1992); Buffels River, a tributary of the Gouritz River in Western Cape (Zawada, 2000); and the Orange River, (Zawada, 2000). The longest available palaeoflood record is that of the lower Orange River, which shows a period of large magnitude flooding between AD 1450 and 1785, during the Little Ice Age (Tyson and Lindesay, 1992). These floods were the largest events of the last 5500 years, reaching magnitudes around three times greater than the largest floods of the instrumental record (Zawada, 2000). Although the lower Orange River borders the northern edge of the Namaqualand region, clearly the flood response of this large basin (ca. 900,000 km^2) reflects hydroclimatic changes upstream in eastern South Africa within the SRZ.

The aim of this paper is to analyse the flood response of the Buffels River, the largest ephemeral river of the Namaqualand region (Northern Cape), to climatic variability during the last millennium based on palaeoflood sedimentary archives in combination with documentary sources and rainfall records. The specific objectives of the paper are to: (1) reconstruct the centennial scale record of flood frequency using the stratigraphic evidence from slackwater flood deposits; (2) compile other sources of non-systematic data (documentary information) and systematic data (rainfall records) to complement the palaeoflood record; and (3) discuss the reconstructed flood record in relation to regional climatic and local environmental changes.

2. Study area

The Buffels River is the largest ephemeral basin in Namaqualand and drains an area of 9250 km^2 into the Atlantic Ocean (Fig. 1). Bedrock underlying the Buffels catchment is composed of impermeable metasedimentary rocks, basic granites and ultrabasic intrusive rocks, cut by basement faults. Average annual precipitation is >300 mm near the Kamiesberg headwaters (1200–1600 m.a.s.l.), 102 mm in the western Bushmanland peneplane (900 m.a.s.l.), 215 mm in the Springbok mountains (1000 m.a.s.l.) and 110 mm at Komaggas on the coastal plain (Fig. 1). Rainfall occurs predominantly in the austral winter, between May and September, and is usually associated with frontal systems from the Atlantic, a situation that has helped determine the existence in the region of a unique winter-rainfall dryland ecosystem (Cowling et al., 1999). Towards the east of Namaqualand, and in the headwaters of the Buffels River catchment, there is a transition to a predominantly summer rainfall regime which is associated with thunderstorms. As a result of this pattern, the majority of floods occur during the winter months although occasional summer rainfall may also cause flash floods. Stream flow records are extremely limited in Namaqualand, a region covering some 45,000 km^2, with one gauge station on the Groen River, located on the southern (Western Cape) border of the Northern Cape, and another on the lower Orange River, an allogenic perennial river with the majority of its drainage area within the SRZ.

Palaeoflood records were reconstructed for three bedrock gorge reaches: Rooifontein and Kamassies in the upper catchment and Messelpad in the lower (Fig. 1). The Rooifontein site (896 km^2) is associated with a fracture in the granite bedrock and is represented by a linear gorge of ca. 7 km in length, 60-120 m wide and 20-30 m deep. Tributaries join the Buffles River at 90º angles, providing optimal settings for slackwater flood deposition (Fig. 1). The bedrock channel is infilled with 1-2 m of sand that is susceptible to scour and fill.

The Kamassies site (drainage area 1422 km^2) is located downstream of the confluence with the Gasab River. Here, the river is incised ca. 4 m into a Pleistocene erosion surface. The river is characterised by an anastomosed channel pattern with levee landforms in areas of overbank deposition. Dense vegetation occurs along the channel and consists mainly of Acacia trees. At the downstream section of the reach, the Buffels River floodplain narrows as it crosses granite bedrock (Fig. 1). In this zone slackwater flood deposits were found on the valley sides and in the lee of bedrock spurs.

The Messelpad site (4956 km^2) represents the optimal of the three palaeoflood study reaches, insofar as bedrock outcrops in the channel bottom providing a stable elevation control. Here the river flows through a gorge (80-100 m wide and over 50 m deep) cut in Mesklip gneiss. The study reach is 400 m long and the channel bed is between 20-40 m wide (Fig. 1).

3. Methodology

Flood hydrological information for the ungauged Buffels River was determined from multiple data sources: a) palaeoflood records derived from slackwater flood stratigraphy (spanning the last millennium); b) documentary records (since AD 1810); and c) instrumental rainfall records (AD 1870-2006). The overlapping timeframes between the different records allowed methodological validation and improved stratigraphic interpretations.

Palaeoflood stratigraphy was determined using standard sedimentological techniques (see Kochel and Baker, 1988 and Benito and Thorndycraft, 2004; 2005 for further details). Flood chronology was provided by radiocarbon and optically stimulated luminescence (OSL) dating (see Tables 1 and 2 for sample details). The radiocarbon dating was done with the AMS (accelerator mass spectrometry) method using the tandem accelerator of the Institute of Particle Physics at the Swiss Federal Institute of Technology, Zurich (ETH). The radiocarbon ages are presented as uncalibrated radiocarbon years BP, and as calendar ages taking the highest probability age range from the 2-sigma calibrated result. The calibration carried out using the CALIB Rev 6.0 software (Stuiver and Reimer, 1993) based on Reimer et al. (2009) calibration data set (Table 1).

The OSL samples (Aitken, 1998) were dated at the luminescence facility of the Israel Geological Survey. Sand samples were collected in the field using PVC cylinders, from which quartz particles with grain sizes of 88-125 µm were extracted from the bulk sediment samples using routine laboratory procedures (Porat, 2006). Approximately 5 mg of the purified quartz was deposited on 10-mm aluminium discs using silicon spray as an adhesive. Single aliquot measurements were done on either a Risø DA-12 or DA-20 TL/OSL reader, equipped with calibrated 90Sr β sources. Quartz stimulation was carried out with a green-filtered halogen bulb or blue LED and detection was through 7-mm U-340 filters. The equivalent dose (De) was determined using the OSL signal and the standard single aliquot regenerative dose (SAR) protocol (Murray and Wintle, 2000), with between 13 and 36 aliquots measured for each sample. Preheats ranged from 220 to 260°C; test dose was 4.5–5 Gy and a cut heat of 180–240°C was used to remove unstable signals. The OSL signal was measured at 125°C to background level. The OSL dates are given as years before 2007, with calendar ages indicated in brackets (see Table 2 for full details).

The two dating methods provided consistent results as indicated by similar ages obtained for samples taken from the same flood unit (e.g., B1-2/11; Tables 1 and 2), as well as the consistency of their stratigraphic order. For sediments older than 200 radiocarbon years, radiocarbon dating generally provided a resolution of ± 50 years, while for younger dates there were increased errors due to the problems inherent in dating young sediments (Trumbore, 2000). For the dating of samples from the last 200 years OSL provided a better resolution, with typical errors of ± 20 to ± 40 years. The combination of both techniques, therefore, provided a means of age control to help constrain flood frequency during the millennia.

The water levels (flood stage) required for deposition of specific stratigraphic flood units were converted into discharge values (O´Connor and Webb, 1988) using the HEC-RAS one dimensional model (Hydrological Engineering Center, 1995). This conversion is an inverse problem, where the minimum discharge (exact water depth above the flood deposit is unknown) is obtained by matching the modelled flood water levels to those obtained in the field from the evidence provided by the elevation of the surveyed flood deposits. Hydraulic modelling requires the estimation of key hydraulic characteristics of the river reaches (energy slope, roughness and cross sectional topography) as well as the boundary conditions upstream or downstream depending on the flow type selected in the model. For this study, subcritical flow conditions were assumed along the surveyed study reach with critical flow selected as the boundary condition. The assigned Manning's *n* values were 0.02-0.025 for unvegetated sandy channels; 0.03-0.035 for sandy bars and margins with disperse vegetation; 0.055-0.1 for sandy bars and margins with dense vegetation; 0.038-0.045 for bedrock slopes and 0.055 for bedrock talus with large boulders. A sensitivity test performed on the model shows that for a 25% variation in the roughness values an error of 1-10% was introduced into the discharge results. The accuracy of the discharge estimates are also dependent on the stability of cross-section topography through time. At the Rooifontein and Kamassies sites in the upper catchment, channel aggradation of 1-2 m has partially filled the bedrock channel with sand deposits susceptible to scour and fill, leading to increased uncertainty on the discharge estimates at these sites.

The palaeoflood data were complemented with instrumental rainfall data compiled from towns within the Buffels catchment (see Fig. 1) and other documentary evidence, an increasingly important source of hydroclimatic data in southern Africa for the 18th and 19th centuries (e.g., Nash and Endfield, 2008). Here, we refer to the documentary records of Kelso and Vogel (2007), compiled from written descriptions at missionary stations. The oldest written record regarding floods or exceptionally high rainfall is from AD 1818, described as a wet year, with severe storms experienced in the Kamiersberg Mountains (Kelso and Vogel, 2007).

4. Results

4.1 Palaeoflood hydrology

4.1.1.Rooifontein

Along this reach the channel bed is typically 20-25 m in width, predominantly composed of coarse sand with trough cross-bedding reflecting lateral bar migration, typical of flat bottomed ephemeral rivers. Six stratigraphic profiles of slackwater flood deposits were described throughout the 600-m reach. The two thickest palaeoflood deposits correspond to flood levees and slackwater sedimentation at tributary junctions (B1-0 and B1-2) approximately 3 m in height above the present channel bed (Fig. 2). Recent flood sediments are common throughout this reach and form during lateral high flow over sand bars (1.5 m above channel bed) on which chute channels are active during flooding (B1-3, B1-4, B1-7, Fig. 1).

The stratigraphic record shows at least 31 flood units, of which 25 were deposited over the last 700 years according to the geochronology. The combination of profiles B1-0 and B1-2 (Fig. 2) provides four stratigraphic sets separated by erosive contacts. The highest flood deposits at profile B1-0 are associated with estimated minimum discharges of 225 m^3s^{-1}. The first set (bottom of B1-0) comprises at least four units (B1-0/9 to 12) of highly bioturbated medium sands. An OSL date sampled from the second unit provided an age of 3500 ± 200 yr. There is a prominent erosive sedimentary contact with the second set of deposits (Fig. 2) which is composed of at least five flood units (B1-0/4 to 8) of fine to very fine sand and silt, each unit characterised by a fining upwards grain size sequence. The lower flood unit (8), exhibiting cross-bedding structures, was OSL dated as 690 ± 70 yr (AD 1250-1390), while the two overlying units (B1-0/6 and 4) were radiocarbon dated as 450 ± 50 and 505 ± 45 ^{14}C yr BP, corresponding to a most likely calibrated age range of AD 1400-1525 and AD 1390-1460, respectively. This second stratigraphic set is associated with a minimum discharge of 150 m^3s^{-1}.

The third stratigraphic set (Fig. 2) is composed of nine flood units (B1-2/4 to 12) of fine to very fine sand and silt. The second lowermost unit (B1-2/11) within this set was OSL dated to 440 ± 40 yr (AD 1530-1610) and radiocarbon dated as 205±50 ^{14}C yr BP (AD 1635-1820). Organic debris found within unit 5 provided a radiocarbon age of 40 ± 45 ^{14}C yr BP (AD 1810-1930). Minimum discharges estimated for this third stratigraphic set range between 100 and 150 m^3s^{-1}. A fourth stratigraphic set comprises between one (B1-0) and three floods (B1-2) deposited between the end of the 19^{th} century and the 20^{th} century, with the highest unit (B1-0/1) likely to correspond to one of the two largest floods of the last 100 years that occurred in AD 1915 and 1925 (Fig. 2). The minimum discharge associated with these events is estimated at 250 m^3s^{-1}.

4.1.2. Kamassies

The floodplain geomorphology shows two alluvial surfaces at 4 and 1.5 m above the channel bed respectively (Fig. 1). The highest bench shows a reworked surface with high flow channels, chute and chute bars related to at least two different stages of evolution. On the upper floodplain surface, three stratigraphic profiles were described (K12, K13, K14). The most complete (K13) is up to 3.5 m in thickness with sixteen flood units identified (Fig. 2). The bottom unit (K13/16) is 0.5 m in thickness and is composed of fine sand with numerous carbonate nodules. An OSL sample provided an age of 730 ± 70 yr (AD 1210-1350). The overlying 10 units (K13/6 to K13/15) are composed of fine to very fine sand containing organic detritus (twigs, charcoal) and silty-clay with dark organic-rich layers accumulated at the top of the sequences. These fine-grained deposits represent alternating sediment fallout and temporal organic accumulation by seasonal vegetation. An OSL date on the upper unit (K13/7) of this middle set provided an age of 330 ± 20 yr (AD 1660-1700). The upper set is composed of five units (K13/1 to K13/5) postdating AD 1700, each with very different characteristics to the earlier deposits with changes in sediment texture (medium to coarse sand), colour (reddish brown) and sedimentary structures (parallel and cross-bedding). These units are related to a period of increasing activity of the chute channels and tractive sedimentation over the floodplain. The minimum discharge required for water flow circulation over the chute channels is 250 m^3s^{-1}.

It is interesting to note that this chronology is repeated on the left bank (K1, K2), where a 2.5-m trench showed a lower set of flood deposits indicating 10 individual events, with a basal OSL age of 800 ± 50 yr (AD 1160-1260; K1/19); and a OSL date of 700 ± 40 yr (AD 1270-1350) from the middle of the sequence (K1/23). A gravel unit marks the contact with the upper sedimentary sequence, which preserves 11 sedimentary units, the oldest of which was radiocarbon dated to 110 ± 45 ^{14}C yr BP (AD 1800-1940). These sediments are characterised by very coarse sand units, usually with basal erosive contacts, that alternate with fine to very fine sand, with ripple marks and evident bioturbation. This bank is overflowed by discharges exceeding 245 m^3s^{-1} for K1 and 210 m^3s^{-1} for K2.

The key sites of slackwater flood deposition at Kamassies were identified in two depositional environments: a small, bedrock protected, valley-side recess on the left margin (K5, K6, K7; Fig. 1); and the lee of a large bedrock spur outcropping in the middle of the canyon (K8, K9, K10). On the bedrock valley side, three inset flood benches at 1.5 m, 2.5 m and 3 m above the channel bed allowed the identification of at least 15 flood units (K5 and K6 in Fig. 2). The upper bench (K5) shows five flood units composed of fine to very fine sand with parallel lamination. Radiocarbon dating on the lower unit (K5/5) provided a radiocarbon age of 530 ± 50 ^{14}C yr BP (AD 1385-1450), and for a middle unit (K5/3) an age of 275 ± 45 ^{14}C yr BP (AD 1475-1675). A minimum discharge of 310 m^3s^{-1} is estimated for deposition on this upper flood bench.

The intermediate and lower benches show similar stratigraphy and contacts, which can be traced following the slope topography. The stratigraphy underlying these benches shows nine flood units (K6, Fig. 2); the upper seven demonstrate high-energy sedimentary structures such as current ripples, dunes, and cross-bedding. Three radiocarbon dates were obtained from these sediments, providing ages of 225 ± 50 ^{14}C yr BP (AD 1510-1830), 115 ± 45 ^{14}C yr BP (AD 1800-1940), and 140 ± 45 ^{14}C yr BP (AD 1670-1895). Minimum discharges of 130 and 220 m^3s^{-1} are associated, respectively, with elevations of the bottom and top flood units of this intermediate bench.

Slackwater flood deposit bench (K9) is located and preserved in the lee of a large bedrock outcrop in the middle of the canyon. The bench is 2.5 m above the channel bed and contains a 2-m-thick sequence representing at least 10 floods (Fig. 3A) deposited over the last 500 years (basal unit K9/10 radiocarbon dated to 360 ± 55 ^{14}C yr BP; AD 1445-1640). The flood units are composed of fine sand and silt, with unit thicknesses ranging from 10–50 cm. In the lower part of this profile, three flood units contain couplets of fine sand and organic enriched layers of 5 to 13 cm in thickness, which are derived from local, temporally ponded environments within these riparian zones (Fig. 3A). A radiocarbon date from the intermediate enriched layer (K9/7) provided an age of 365 ± 50 ^{14}C yr BP (AD 1450-1640) indicating a rapid aggradation of the lower part of the profile. Within the upper five flood units the texture increased to fine and medium sands that included tractive structures (current ripples and trough cross beds), parallel laminations, and massive structure. The flood units are capped by enriched organic laminae, dated in the second upper flood unit (K9/2) with a radiocarbon age of 160 ± 45 ^{14}C yr BP (AD 1715-1890) (Fig. 3A). The minimum flood discharges matching the elevation of the bottom and top flood units are 100 and 260 m^3s^{-1}, respectively.

4.1.3. Messelpad

Here, the slackwater flood deposits are emplaced on the left valley margin where a large rock fall (with boulders over 7 m in diameter), and bedrock outcrops favored the development of eddy flow during floods (Fig. 3C). The flood deposits form two benches at +4.5 m and +1.5-2 m above the channel bed. The oldest flood deposits found within the Buffels River catchment are from the slackwater flood deposits found at profile BM-9 where there is evidence for three floods deposited before the first millennia BC; two associated with a radiocarbon age of 2880±50 ^{14}C yr BP (1255-920 BC); and a further two floods postdating a radiocarbon calibrated age of AD 640-785 (Fig. 3B).

Eight stratigraphic profiles up to 2.5 m in thickness preserved sedimentary evidence for at least 21 flood events over the last 300 years. Several flood units show clear stratigraphic correlation between five stratigraphic profiles, three within the middle part of the reach (BM1, BM2, and BM3), and two 75 m upstream (BM7, BM8). The stratigraphic correlation shows two main depositional sets (Fig. 2). The oldest one, at the base of the profile, comprises a colluvium (sands with dispersed pebble grains) and one flood unit (fine sand with parallel lamination) radiocarbon dated to 395±60 ^{14}C yr BP (AD 1430-1640). The second set comprises eleven flood units, five of which were deposited only in profile BM8, whereas the other six are also present at profiles BM1, BM2, BM3 and BM7. These units are about 10 cm in thickness and are composed by couplets of sand, with parallel lamination and/or ripples (2-8 cm), and organic detritus (1-3 cm). Another stratigraphic marker, traced throughout the study reach, is a unit of fine and very fine sand, reaching 40-50 cm in thickness, with climbing ripples indicating both upstream and downstream flow direction (reflecting eddy circulation), and parallel lamination with organic detrital laminae (Fig. 3D). In these six flood units two radiocarbon dates provided ages of 25 ± 45 ^{14}C yr BP (AD 1810-1925) and 95 ± 45 ^{14}C yr BP (AD 1800-1940). The highest elevation flood deposits here are associated with an estimated minimum discharge of 510 m^3s^{-1} (profile BM7; Fig. 3C). At least seven floods provided a minimum discharge of 400 m^3s^{-1}, five between minima of 200 and 400 m^3s^{-1}, and at least 10 showed a minimum discharge lower than 100 m^3s^{-1}.

The lower flood bench (+1.5 m above the channel bed) contains at least 16 flood units, 10 of which postdate a modern radiocarbon age. The other six, at the base of the bench, contain carbonate nodules and iron oxide mottles, which are indicative of high water-table conditions.

4.2 Documentary and Historical flood records

The documentary record reported by Kelso and Vogel (2007) provides a proxy precipitation data set for Namaqualand for the 19th century and enables the detection of periods of increased rainfall and drought (Fig. 4). Documentary data were tested over the period 1878-1900 against the earliest instrumental rainfall at Springbok. Kelso and Vogel (2007) provided a yearly classification of relative rainfall conditions since 1817, considering drought years to be those with <75% of mean annual rainfall, with wet years classified according to >125 % annual rainfall (Vogel et al., 2000). Figure 4 shows the Springbok rainfall station record since 1878 and transformation of the Kelso and Vogel classification to rainfall anomaly classes for illustrative purposes, using the following definitions: -2 drought year; -1 dry year; +0.5 normal year; +2 wet year. Years with insufficient evidence are not plotted.

The oldest written reference to high rainfall describes 1818 as a wet year, with severe storm(s) being experienced in the Kamiersberg area (Kelso and Vogel 2007 citing the Wesleyan Methodist Missionary Society, 1819). Heavy rains were reported in the winter of 1822 (Kelso and Vogel, 2007) with devastating effects in Leliefontein. Apart from 1818, other years with good winter rains corresponded to AD 1822-1823, 1831, 1859, 1872, 1878, 1888, 1899 and 1900. Documentary records indicate AD 1888 as a year with exceptional winter rainfalls during which ephemeral rivers flowed for some months (Kelso and Vogel, 2007). This is corroborated by rainfall instrumental data recorded in Springbok, with the year 1888 registering the third largest winter precipitation on record (394 mm: 94% of annual rainfall). During the 20th century, the winter precipitation ranking in Springbok is headed by 1915 (454 mm) followed by 1925 (427 mm), 1921 (346 mm), 1917 (311 mm) and 1920 (297 mm), making 1915-1925 the wettest 10-yr period on record with respect to winter rainfall. This period also coincides with the largest 20th century floods according to oral history from the Kamassies and Rooifontein villages (Fig. 1). Following this period, there was a significant shift towards decreasing precipitation. The 90th-percentile winter rainfall (~240 mm), the value which, when exceeded, results in large flooding of the Buffels River, was only reached in 1996 (325 mm), 1963 (284 mm), 1930 (269 mm), 1939 (244 mm), 1941 (243.8) and 1997 (242 mm). The winter rainfall series in Springbok shows a slightly increasing trend in annual total precipitation since 1991.

5. Discussion

Although the earliest palaeoflood deposits of the Buffels River, found at Messelpad, were dated to the first millennium BC (Fig. 3B), the three study reaches provide a common 700-yr time frame for investigating the occurrence and minimum magnitudes of the largest floods of this ephemeral river. Figure 5 shows individual palaeofloods for the study reaches, with vertical black bars designating floods dated either by radiocarbon or OSL techniques. Horizontal bars show the 2-sigma (68%) age uncertainty. For high age uncertainty, estimated palaeoflood age was placed at the midpoint of the calibration sector representing the highest age probability (e.g., samples BM7/5, and K6/7, Table 1); otherwise, the midpoint of the 2-sigma calibration interval was used. Vertical blue bars represent undated stratigraphic units. A tentative age was assigned to each sedimentary flood unit considering: 1) bracketing age intervals within the stratigraphic section; and 2) the stratigraphic record and dated flood deposits at all three sites, based on the assumption that high magnitude floods were generated at the basin scale. During the period of overlapping documentary and instrumental records (since AD 1800) the assigned palaeoflood age was based on documented flood years with the bracketing ages provided by the dated geochronology. In Figure 5, light brown shaded areas show the minimum discharge for the specified time periods required for emplacing a new deposit on top of the flood bench. The pre-1600s palaeoflood stratigraphic record at both Kamassies and Messelpad mainly captured the more extreme events, while a more complete record for this period is preserved at Rooifontein. By contrast, the post-1600s stratigraphic record of large floods is better preserved at the Kamassies and Messelpad reaches.

Collectively, the reconstructed palaeoflood record (Fig. 6) indicates large-magnitude floods were more frequent during AD 1390-1425 and AD 1800-1825. These floods generally surpassed a minimum discharge threshold of 255 m^3s^{-1} in the upper catchment and 510 m^3s^{-1} in the lower catchment. The combined instrumental, documentary and palaeoflood data for the 20th century indicate a third flood episode (> 4 events) from AD 1915 to AD 1925. The cluster of high rainfall and flooding during 1915-1925 is associated with a large winter precipitation anomaly and is suggested as an analogue for previous flood episodes preserved in the sedimentary record. The period 1600-1800 shows occasional occurrences of large floods, with an average cumulative frequency for the 700 years covered by the record. During AD 1425-1600 and AD 1825-1915 few large floods were recorded (e.g., *ca* AD 1526 and AD 1888).

Long-term (centennial) high-resolution climatic records in southern Africa are scarce. However, quasi-decadal-resolution oxygen and stable carbon isotope data derived from a speleothem recovered from Cold Air Cave in Makapansgat Valley (northeast South Africa, ~1500 km northeast of our study area) provide the most accurate climate proxy records for the summer-rainfall region (Holmgren et al., 1999, Fig. 6). Here variations in oxygen and carbon isotopes over the last 3000 years reveal five centuries of colder conditions associated with the Little Ice Age from AD 1300 to 1800 (Holmgren et al., 1999, Tyson et al., 2000). In particular, the coldest phases in South Africa occurred during AD 1300-1500 and AD 1675-1780 (Tyson and Lindesay, 1992), with the greatest cooling severity occurring around AD 1700 when there was a ~2°C decrease in mean temperature (Holmgren et al., 1999; Tyson et al., 2000). The first cold phase within the LIA brackets a period of frequent large floods in the Buffels River (AD 1390-1425, Fig. 6). The second cold phase (AD 1675-1780) corresponds with the Late Maunder Minimum (AD 1675-1715), when there was reduced solar activity (Tyson et al., 2000). It is interesting to note that over the Late Maunder Minimum, large floods occurred regularly though with no apparent increase in decadal-scale flood frequency (~3 floods in 100 years). By contrast, however, the Spörer Minimum (about AD 1420-1570) was not found to be associated with flooding in the Buffels River. Periods of higher frequency of large floods (AD 1390-1425, AD 1800-1825 and AD 1915-1925) occurred within a decadal timeframe (~4-5 large floods in 20-30 years), most likely associated with shifts in atmospheric circulation. Conversely, the lowest frequency of large floods (~1 large flood in 100 years; at AD1425-1600) seems to be associated with prevailing warmer conditions.

Tyson and Lindesay (1992) and Tyson (1993) proposed a hydroclimatic model for southern Africa relating cold periods of the LIA with wetter conditions within the winter-rainfall regions and reduced precipitation in the summer-rainfall region (see Fig. 1 for rainfall regime areas in southern Africa). Increased temperature during times dominated by tropical circulation regimes also contributed to increased dryness in the winter-rainfall area and wetter conditions in the summer-rainfall region. According to Zawada (2000) this hydroclimatic model explains the palaeoflood chronology of the Orange River fed by summer rains, with the warmer phases of the LIA (in particular AD 1500 to 1675, after Tyson, 1993) accounting for the largest palaeoflood discharges of the last 5500 years.

In the Buffels River, within the northern limit of the winter-rainfall region, it is difficult to precisely determine flood response to climatic variability given the contrasting resolutions of the palaeoflood and Makapansgat Valley stalagmite records (Fig. 6). The palaeoflood record generally shows a sustained frequency of large floods during cold episodes (e.g., AD 1600-1800) and a decreasing occurrence of large floods during warmer conditions (e.g., 1425-1600 and after 1925). However, the highest frequency of large floods occurred at times of transition between climate episodes as evident by comparison of $\delta^{18}O$ changes against numbers of large and medium size floods (Fig. 6). Apparently these climatic transitions involve more frequent and intense frontal systems associated with Atlantic westerlies (Cockcroft et al., 1987; Chase and Meadows, 2007). Anomalous wet winters are currently associated with negative pressure anomalies of the Antarctic Oscillation (AAO) or Southern Annular Mode that may persist into the following spring season (Reason and Rouault, 2005). Most wet winters over the instrumental record (1950-2000) tended to be associated with high temperature gradients in the central South Atlantic sector, which results from anomalously warm SST in the SW Atlantic and SE Atlantic and increased sea-ice extent in the Southern Ocean (Reason et al., 2002). Consequently, periods of high frequency of large floods in the Buffels River may reflect decadal episodes of anomalous negative persistence of the AAO, indicative of strong temperature gradients across the Southern Ocean.

Both the long-term palaeoflood data and the flood record compiled from historical information and rainfall data indicate that the 20th century witnessed a reduction in the frequency of large floods in the Buffels River system. This decrease in frequency of large floods since 1930 can be linked to gradual warming and to the general trend of decreasing rainfall following the Little Ice Age. The analysis of 50-year (1950-1999) observed rainfall data for the region shows a general decreasing trend in winter precipitation (June-August), the main rainfall season, with an increase in convective rainfall during March to May (MacKellar et al., 2007). Future climate projections, based on GCM simulations forced with the SRES A2 and A1B emissions scenarios (Nakićenović et al., 2000), predict by 2050 a 3-4 degree rise in temperature (Christensen et al., 2007), a 25% drop in winter rainfall (Hulme et al., 2001; Midgley et al. 2005; MacKellar et al., 2007), and subsequently reduced runoff of 10-20%, relative to the period 1900-1970 (Milly et al., 2005). This suggests that with future global warming there may be fewer large floods in the region. The question of how a reduced frequency of large floods will impact the hydrology of the Buffels River, water resources, biodiversity and livelihoods of the local population is under investigation (Hoffman and Rohde, 2007, 2010).

6. Summary and conclusions

This paper presented a long-term flood history, based on multiple data sources, for the ungauged Buffels River, the largest ephemeral river of Namaqualand (South Africa), with the aim of improving our understanding of flood magnitude and frequency relationships in ephemeral river hydrology, where climate variability is a major controlling factor. Flood data during the pre-instrumental period were retrieved from a combination of documentary descriptions at missionary stations and sedimentary evidence (slack-water flood sediments) using palaeoflood hydrological techniques. The combined methodology resulted in recognition of more than 25 major floods over the last 700 years. The aggregate record is based on the assumption that the largest floods occurred simultaneously throughout the catchment and their preservation in the stratigraphic record depends on flood levels exceeding the elevation of previous flood deposits (censored records). Ages of individual palaeofloods were estimated by radiocarbon and OSL dating which provided a sub-centennial resolution. Documentary records gave a yearly resolution for the largest floods of the 19th century, which also were recorded in the stratigraphic record.

Large floods occurred throughout the palaeoflood record; however, they occurred with higher frequency during AD 1390-1425, 1800-1825, and 1915-1925. The highest magnitude floods in the upper catchment reached a minimum discharge of 255 m^3s^{-1}, whereas the minimum estimated flood discharge in the lower downstream basin was 510 m^3s^{-1}. The magnitude and frequency of extreme floods appears to have decreased since the 1930s, in association with an observed decrease in rainfall for this period. Increased flood magnitudes and/or frequencies in the Buffels River are hypothesised to be favoured when winter frontal systems are displaced equatorwards from their normal seasonal locations. Such displacement seems more likely to reach Namaqualand's latitude during shifts in climatic conditions at decadal scales inducing changes in the flood frequency of the Buffels river basin. During the most severe cooling episode of the Little Ice Age at AD 1675-1780, anomalous rainfall produced large floods in the Buffels basin, although within normal recurrence intervals (~3 floods in 100 years).

Palaeoflood records from the Buffels River catchment suggest that large floods coincided in the past within two prevailing climatic scenarios: periods of regular large flood occurrence (1 large flood/~30 yrs) under wetter and cooler prevailing climatic conditions (AD 1600-1800), and periods of high frequency of large floods coinciding with wetter conditions of decadal duration (e.g., the early 20th century episode of large floods between 1915-1925). These decadal high-frequency flooding (~4-5 large floods in 20-30 years) periods may point out changes on atmospheric circulation involving more frequent and intense frontal systems, currently associated with strong temperature gradients across the Southern Ocean.

The mid- and late 20th century has had significantly fewer large flood events. The lower frequency of larger floods together with a general trend in decreasing winter rainfall in Namaqualand since the early 20th century are indicative of the expected flood response to increased global warming in the region (Christensen et al., 2007), and in agreement with GCM simulations performed for Namaqualand (MacKellar et al., 2007). At the global scale this paper adds to a growing list of basin-scale research that stresses the role of changing circulation patterns, as opposed to the moisture-holding capacity of the atmosphere, in driving flood response to climatic variability (e.g., Knox, 2000; Thorndycraft et al., 2005; Thorndycraft and Benito, 2006).

Acknowledgments

The study was funded by the 6th Framework Programme of the European Commission through the project “FloodWater recharge of alluvial Aquifers in Dryland Environments”, WADE Project (contract no. GOCE-CT-2003-506680). Daferey Waldeck (Rooifontein) Anna Marie Boyce (Buffelsrivier) and Penny Price (University of Cape Town) are gratefully thanked for their field assistance. We are very grateful to Michael Davis and Naomi Porat at the Luminescence Lab of the Geological Survey of Israel (Jerusalem) for processing and interpreting the OSL datings. We appreciate the manuscript review and comments provided by Jim Knox (University of Wisconsin-Madison) and two anonymous reviewers.

References

Aitken, M.J. 1998. An Introduction to Optical Dating. The Dating of Quaternary Sediments by the Use of Photon-stimulated Luminescence. Oxford University Press, Oxford. 280pp.

Benito, G., Thorndycraft, V.R., 2004 (Eds.). Systematic, palaeoflood and historical data for the improvement of flood risk estimation. Methodological Guidelines. CSIC, Madrid. 115 pp.

Benito G., Thorndycraft V.R., 2005. Palaeoflood hydrology and its role in applied hydrological sciences. Journal of Hydrology 313, 3-15.

Benito, G., Rohde, R., Seely, M., Külls, C., Dahan, O., Enzel, Y., Todd, S., Botero, B., Morin, E., Grodek, T., Roberts, C., 2010. Management of Alluvial Aquifers in Two Southern African Ephemeral Rivers: Implications for IWRM. Water Resources Management 24, 641–667.

Benito, G., Thorndycraft, V.R., Rico, M., Sánchez-Moya, Y., Sopeña, A., 2008. Palaeoflood and floodplain records from Spain: Evidence for long-term climate variability and environmental changes. Geomorphology 101, 68–77.

Chase, B.M., Meadows, M.E., 2007. Late Quaternary dynamics of southern Africa's winter rainfall zone. Earth-Science Reviews 84, 103-138.

Christensen, J.H., Hewitson, B., Busuioc, A., Chen, A., Gao, X., Held, I., Jones, R., Kolli, R.K., Kwon, W.-T., Laprise, R., Magaña Rueda, V., Mearns, L., Menéndez, C.G., Räisänen, J., Rinke, A., Sarr, A. and Whetton, P., 2007. Regional Climate Projections. In: Solomon, S., Qin, D., Manning, M., Chen, Z., Marquis, M., Averyt, K.B., Tignor, M. and Miller, H.L. (eds.). Climate Change 2007: The Physical Science Basis. Contribution of Working Group I to the Fourth Assessment Report of the Intergovernmental Panel on Climate Change Cambridge University Press, Cambridge, United Kingdom and New York, NY, USA, pp. 847-940.

Cockcroft, M.J., Wilkinson, M.J., Tyson, P.D., 1987. The application of a present-day climatic model to the late Quaternary in southern Africa. Climatic Change 10, 161-181.

Cowling, R.M., Esler, K.J., Rundel, P.W., 1999. Namaqualand, South Africa – an overview of a unique winter-rainfall desert ecosystem. Plant Ecology 142(1-2), 3-21.

Desmet, P.G., 2007. Namaqualand--A brief overview of the physical and floristic environment. Journal of Arid Environments 70, 570-587

Ely, L.L., Enzel, Y., Baker, V.R., Cayan, D.R., 1993. A 5000-year record of extreme floods and climate change in the southwestern United States. Science 262, 410-412.

Hirschboeck, K.K., 1988. Flood hydroclimatology. In: Baker, V.R., Kochel R.C., Patton P.C. (Eds). Flood Geomorphology. John Wiley & Sons, New York, pp. 27-49.

Hoffman, M.T., Rohde, R.F., 2007. From pastoralism to tourism: The historical impact of changing land use practices in Namaqualand. Journal of Arid Environments 70, 641-658.

Hoffman, M.T., Rohde, R.F., 2010. Rivers through time: Historical changes in the riparian vegetation of the semi-arid, winter rainfall region of South Africa in response to climate and land use. Journal of the History of Biology (in press).

Holmgren, K., Karlén, W., Lauritzen, S.E., Lee–Thorp, J.A., Partridge, T.C., Piketh, S., Repinski, P., Stevenson, C., Svanered, O. and Tyson, P.D., 1999. A 3000-year high-resolution stalagmite based record of palaeoclimate for northeastern South Africa. The Holocene 9, 295–309.

Holmgren, K., Lee-Thorp, J.A., Cooper, G.R.J., Lundblad, K., Partridge, T.C., Scott, L., Sithaldeen, R., Talma, A.S. and Tyson, P.D., 2003. Persistent millennial-scale climatic variability over the past 25,000 years in Southern Africa. Quaternary Science Reviews 22, 2311-2326.

Hulme, M., Doherty, R., Ngara, T., New, M., Lister, D., 2001. African climate change: 1900–2100. Climate Research 17, 145–168.

Hydrologic Engineering Center, 1995. HEC-RAS, River Analysis System, Hydraulics Reference Manual, (CPD-69). Davis, California.

Kelso, C., Vogel, C., 2007. The climate of Namaqualand in the nineteenth century. Climatic Change 83, 357-380.

Knox, J.C., 2000. Sensitivity of modern and Holocene floods to climate change. Quaternary Science Reviews 19, 439-457.

Kochel, R.C., Baker V.R., 1988. Paleoflood analysis using slack water deposits. In: Baker, R.V, Kochel, R.C., Patton, P.C. (Eds). Flood Geomorphology. Wiley Interscience, New York, pp. 357-376.

MacKellar, N.C., Hewitson, B.C., Tadross, M.A., 2007. Namaqualand's climate: Recent historical changes and future scenarios. Journal of Arid Environments 70, 604-614.

Midgley, G.F., Thuiller, W., 2007. Could anthropogenic climate change threaten biodiversity in Namaqualand? Journal of Arid Environments 70, 615-628.

Midgley, G.F., Chapman, R.A., Hewitson, B., Johnston, P., De Wit, M., Ziervogel, G., Mukheibir, P., Van Niekerk, L., Tadross, M., Van Wilgen, B.W., Kgope, B., Morant, P., Theron, A., Scholes, R.J. & Forsyth, G.G., 2005. A Status Quo, Vulnerability and Adaptation Assessment of the Physical and Socio-Economic Effects of Climate Change in the Western Cape, Report to the Western Cape Government, Cape Town, South Africa. Report No. ENV-S-C 2005-073. Stellenbosch, CSIR.

Milly, P.C.D., Wetherald, R.T., Dunne, K.A., Delworth, T.L. 2002. Increasing risk of great floods in a changing climate. Nature 415, 514–517.

Milly, P.C.D., Dunne, K.A., Vecchia, A.V., 2005. Global pattern of trends in streamflow and water availability in a changing climate. Nature 438, 347-350.

Morin, E., Grodek, T., Dahan, O., Benito, G., Kulls, C., Jacoby, Y.Van Langenhove, G., Seely, M., Enzel, Y., 2009. Flood routing and alluvial aquifer recharge along the ephemeral arid Kuiseb River, Namibia. Journal of Hydrology 368, 262–275

Murray, A., Wintle, A.G., 2000. Luminescence dating of quartz using an improved single-aliquot regererative-dose protocol. Radiat. Meas. 32, 57–73.

Nakićenović N., Alcamo J., Davis G., De Vries B., Fenhann, J. Gaffin, S. Gregory K., Grübler A., Jung T.Y., Kram T., La Rovere E.L., Michealis L., Mori S., Morita T., Pepper W., Pitcher H., Price L., Raihi K., Roehrl, A. Rogner H.-H., Sankovski A., Schlesinger M., Shukla P., Smith S., Swart, R. Van Rooijen S., Victor N., Dadi Z., 2000. IPCC Special Report on Emission Scenarios. Cambridge University Press, Cambridge, UK, 599pp.

Nash, D.J., Endfield, G.H., 2008. 'Splendid rains have fallen': links between El Niño and rainfall variability in the Kalahari, 1840–1900. Climatic Change 86, 257-290.

O'Connor, J.E., Webb, R.H., 1988. Hydraulic Modeling for Palaeoflood Analysis. In: Baker, V.R., Kochel, R.C., Patton, P.C. (Eds.), Flood Geomorphology, John Wiley and Sons, New York, pp. 393-403.

Porat, N., 2006. Use of magnetic separation for purifying quartz for luminescence dating. Ancient TL 24, 33–36.

Reason, C.J.C., Rouault, M., 2005. Links between the Antarctic Oscillation and winter rainfall over western South Africa. Geophysical Research Letters 32, L07705, doi:10.1029/2005GL022419.

Reason, C.J.C., Rouault, M., Melice, J.L., Jagadheesha, D., 2002. Interannual winter rainfall variability in SW South Africa and large scale ocean-atmosphere interactions. Meteorology and Atmospheric Physics 80, 19-29.

Redmond, K.T., Enzel, Y., House, P.K. Biondi, F., 2002. Climate variability and flood frequency at decadal to millennial time scales. In: House P.K., Webb R.H., Baker V.R., Levish D.R. (Eds.). Ancient floods, modern hazards: Principles and applications of Paleoflood Hydrology. Water Science and Application vol. 5, American Geophysical Union, Washington DC. pp. 21-45.

Reimer, P.J., Baillie, M.G.L., Bard, E., Bayliss, A., Beck, J.W., Blackwell, P.G., Bronk Ramsey, C., Buck, C.E., Burr, G.S., Edwards, R.L., Friedrich, M., Grootes, P.M., Guilderson, T.P., HajdasI, I., Heaton, T.J., Hogg, A.G., Hughen, K.A., Kaiser, K.F., Kromer, B., McCormac, F.G., Manning, S.W., Reimer, R.W., Richards, D.A., Southon, J.R., Talamo, S., Turney, C.S.M., van der Plicht, J., Weyhenmeyer, C.E., 2009. IntCal09 and Marine09 radiocarbon age calibration curves, 0-50,000 years cal BP. Radiocarbon 51, 1111-1150.

Schick, A.P., 1988. Hydrologic aspects of floods in extreme arid environments. In: Baker, V.R., Kochel, R.C., Patton P.C. (Eds.), Flood Geomorphology. Wiley Interscience, New York, pp. 189-203.

Smith, A.M., 1992. Palaeoflood hydrology of the lower Umgeni River from a reach south of the Inanda Dam, Natal. South Africa Geographical Journal 74, 63-68.

Smith, A.M., Zawada, P.K., 1990. Palaeoflood hydrology: A tool for South Africa? — An example from the Crocodile River near Brits, Transvaal, South Africa. Water SA 16, 195-200.

Stuiver, M., Reimer, P.J., 1993. Extended 14C database and revised CALIB radiocarbon calibration program, Radiocarbon 35, 215-230.

Thorndycraft V.R., Benito G., 2006. The Holocene fluvial chronology of Spain: Evidence from a newly compiled radiocarbon database. Quaternary Science Reviews 25, 223-234.

Thorndycraft V.R., Benito G., Rico M., Sánchez-Moya Y., Sopeña A., Casas A. 2005. A long-term flood discharge record derived from slackwater flood deposits of the Llobregat River, NE Spain. Journal of Hydrology 313, 16-31.

Tooth, S., 2000. Process, form and change in dryland rivers: a review of recent research. Earth-Science Reviews 51, 67-107.

Trenberth, K.E., Jones, P.D., Ambenje, P., Bojariu, R., Easterling, D., Klein Tank, A., Parker, D., Rahimzadeh, F., Renwick, J.A., Rusticucci, M., Soden, B., Zhai, P., 2007. Observations: Surface and Atmospheric Climate Change. In: Solomon, S., Qin, D., Manning, M., Chen, Z., Marquis, M., Averyt, K.B., Tignor, M., Miller, H.L. (eds.), Climate Change 2007: The Physical Science Basis. Contribution of Working Group I to the Fourth Assessment Report of the Intergovernmental Panel on Climate Change. Cambridge University Press, Cambridge, United Kingdom and New York, NY, USA, pp. 235-336.

Trumbore, S.E., 2000, Radiocarbon geochronology. In: Noller J.S., Sowers J.M., Lettis W.R. (eds.), Quaternary Geochronology: Methods and Applications, American Geophysical Union, New York, pp. 41-60.

Tyson P.D., Karlén W., Holmgren K., Heiss, G.A., 2000. The Little Ice Age and Medieval Warming in South Africa. South African Journal of Science 96, 121-126

Tyson, P.D. 1999. Late Quaternary and Holocene palaeoclimates of southern Africa: A synthesis. South African Journal of Geology 102, 335-349.

Tyson, P.D., Lindesay, J.A., 1992. The climate of the last 2000 years in southern Africa. The Holocene 2, 271–278.

Tyson, P.D., 1993. Recent developments in the modelling of the future climate of southern Africa. South African Journal of Science 89, 494–505.

Vogel, C., Laing, M., Monnik, K., 2000. Drought in Southern Africa, with special reference to the 1980-1994 period. In: Wilhite, D.A. (ed.). Drought volume 1: A global assessment, Routledge Hazar and Disaster Series, London, pp. 348-366.

Zawada, P.K., 2000. Palaeoflood hydrological analysis of selected South African rivers. Memoir of the Council for Geoscience, South Africa, Memoir 87, 173 pp.

Figure captions

Figure 1. Upper: The Buffels River catchment showing the major drainage network, palaeoflood sites (circle-R: Rooifontein, circle-K: Kamassies and circle-M: Messelpad) and rainfall isohyets. Inset: Location of the study area within South Africa and indication of the rainfall regime zones. MV indicates the location of the proxy records from stalagmites in the Makapansgat Valley. Lower: Geomorphological sketch maps of the study reaches and location of stratigraphic profiles containing slackwater flood deposits.

Figure 2. Stratigraphic profiles of the key sedimentary profiles at the three study reaches indicating dated samples (radiocarbon dates in conventional ^{14}C years BP) and proposed correlations between sections.

Figure 3. A: View of the K9 stratigraphic profile in Kamassies showing a sequence of slackwater flood deposition reaching a thickness of ca. 2 m. B: View of the BM9 pit in Messelpad with indication of the stratigraphic units and radiocarbon dating results. C: General view of the upper section of the Messelpad study reach and location of three profiles (note people inside the circle for scale). D: Lower part of slackwater unit 3 in BM8 profile (Messelpad) showing an organic detrital laminae and climbing ripples with both upstream and downstream flow direction (indicative of eddy circulation).

Figure 4. Rainfall record at the Springbok rain station (black line) and rainfall anomaly classes (red bars: drought/dry years; blue bars: wet/normal years) from documentary records after Kelso and Vogel (2007). Rainfall anomaly class values are only for

illustrative purposes: -2 drought year, -1 dry year, +0.5 normal year; +2 wet year. Years with insufficient evidence are not plotted. Documented flood years are indicated in the upper *x* axis.

Figure 5. Schematic diagrams showing the interpreted flood records of the study reaches based on palaeoflood, historical flood and systematic rainfall data. Light brown shaded areas indicate censored flood records during the non-systematic period; i.e., only flood stages exceeding in elevation the top of the deposit emplaced by previous large floods were recorded. Conversely, floods with peak discharges less than the censoring level were not recorded. Black bars show minimum discharge estimates of individual floods dated in the stratigraphic record at the site, represented as midpoint calibrated and OSL years AD (Tables 1 and 2), with 2-sigma geochronological age uncertainties indicated by the horizontal lines. Blue bars are minimum discharge estimates of non-dated depositional flood units at the site, with a tentatively assigned age based on bracketed ages from other flood sites and/or known flood years from documentary records.

Figure 6. Upper: Oxygen stable isotope data of Cold Air Cave Stalagmite from the Makapansgat Valley (Holmgren et al., 2003 in IGBP PAGES/World Data Center for Paleoclimatology, Contribution # 2005-034). Lower: Accumulated number of palaeofloods (large floods) based on palaeoflood stratigraphic records dated with radiocarbon and OSL (white colour circles), and documented (black circles) medium to large magnitude floods (not included in palaeoflood record). Shaded areas (numbers 1, 3 and 4) denote times with increased frequencies of large floods and the shaded area with a white oblique pattern (period number 2) represent and extended period of relatively

lower frequencies of large floods during a cooling episode of the Little Ice Age as indicated by the decreased isotopic values of $\delta^{18}O$.

Table 1. Radiocarbon dating samples and results, including calibrated ages calculated by the CALIB Rev 6.0 software (Stuiver and Reimer, 1993) using the calibration data set of Reimer et al. (2009).

Table 2. Optically stimulated luminescence dating results from slackwater flood deposits in the Buffels River. Samples have recycling ratios mostly within 5% of 1.0. IRSL consist of less than 5% of the OSL signal. The α, β and γ dose rates were calculated from the concentrations of the radioisotopes (K, U, Th) and the cosmic dose rates estimated from burial depths. The α contribution is 30-60 μGy/a (not in Table). Water content estimated at 5±2%. [a]Number of aliquots measured for each sample used to calculate the mean, from a total number of preparations (in parentheses). [b] De: Equivalent dose (Gy). [c] Radiocarbon date from sample taken in the same stratigraphic unit. [d] 23 small aliquots (100-200 grains) were also measured for sample BFL-2 and their results were combined with the regular measurements. There is a bimodal distribution of De values, which may indicate poorly bleached grains. Ages are shown for both groups.

Table 1

Flood unit	Sample material	Lab code	Age, ^{14}C yrs BP	Calibrated age range (2σ), yr BP	Calibrated age range, AD	Most likely age range, AD
			Rooifontein reach			
B1-0/6	Charcoal	UZ-5265/ ETH-31153	450±50	552-426 380-319	1398-1524 (89%) 1570-1631 (10%)	1400-1525
B1-0/4	Charcoal	UZ-5266/ ETH-31154	505±45	563-491 637-593	1387-1459 (83%) 1313-1357 (17%)	1390-1460
B1-0/2	Seed	UZ-5267/ ETH-31155	Modern			
B1-2/11	Charcoal	UZ-5280/ ETH-31493	205±50	232-122 317-241 40-0	1718-1818 (46%) 1633-1709 (27%) 1910-1950 (16%)	1635-1820
B1-2/5	Wood	UZ-5281/ ETH-31494	40±45	142-23 265-219	1808-1927 (73%) 1685-1731 (25%)	1810-1930
B1-4/3	Twigs	UZ-5268/ ETH-31156	Modern			
B1-4/11	Charcoal	UZ-5269/ ETH-31157	Modern			
			Kamassies reach			
K1/11	Charcoal	UZ-5293/ ETH-31506	110±45	151-9 274-182	1799-1941 (63%) 1676-1768 (34%)	1800-1940
K5/3	Charcoal	UZ-5292/ ETH-31505	275±45	477-274 173-0	1473-1676 (91%) 1777-1951 (8%)	1475-1675
K5/5	Charcoal	UZ-5272/ ETH-31175	530±50	567-502 648-584	1383-1448 (63%) 1302-1366 (37%)	1385-1450
K6/3	Rodent coprolite	UZ-5273/ ETH-31176	140±45	283-168 154-56 46-0	1667-1782 (44%) 1796-1894 (38%) 1904-1953 (18%)	1670-1895
K6/5	Charcoal	UZ-5274/ ETH-31177	115±45	151-9 275-173	1799-1941 (62%) 1675-1777 (37%)	1800-1940
K6/7	Organic silt	UZ-5275/ ETH-31178	225±60	438-123 119-0	1512-1827 (80%) 1831-1953 (19%)	1510-1830
K9/10	Charcoal	UZ-5278/ ETH-31181	360±55	504-308	1446-1642 (100%)	1445-1640
K9/7	Charcoal	UZ-5277/ ETH-31180	365±50	503-312	1447-1638 (100%)	1450-1640
K9/2	Charcoal	UZ-5276/ ETH-31179	160±45	234-59 288-238 42-0	1716-1891 (64%) 1662-1712 (18%) 1908-1953 (18%)	1715-1890
			Messelpad reach			
BM2-5	Charcoal	UZ-5282/ ETH-31495	395±60	520-312	1430-1638 (100%)	1430-1640
BM3-3	Charcoal	UZ-5283/ ETH-31496	95±45	150-11 271-186	1800-1939 (67%) 1679-1764 (32%)	1800-1940

BM3-5	Charcoal	UZ-5284/ ETH-31497	25±45	140-25 260-221	1810-1925 (74%) 1690-1729 (24%)	1810-1925
BM4-4	Charcoal	UZ-5285/ ETH-31498	Modern			
BM5-6	Charcoal	UZ-5286/ ETH-31499	Modern			
BM9-4	Charcoal	UZ-5270/ ETH-31158	1315±50	1313-1167 1163-1090	637-783 (95%) 787-860 (5%)	640-785
BM9-10	Charcoal	UZ-5287/ ETH-31500	2880±50	3202-2870	BC 1253-921 (100%)	BC 1255-920
			Eselsfontein reach			
EF1/4	Charcoal	UZ-5288/ ETH-31501	485±45	560-465 631-599	1390-1485 (93%) 1319-1351 (7%)	1390-1485
EF3/5	Twigs	UZ-5289/ ETH-31502	155±95	324-0 428-376	1626-1954 (96%) 1522-1574 (4%)	1625-1950
EF5/5	Charcoal	UZ-5290/ ETH-31503	35±45	141-24 263-220	1809-1926 (73%) 1687-1730 (25%)	1810-1925
EF5/7	Charcoal	UZ-5291/ ETH-31504	135±45	153-2 282-169	1797-1948 (56%) 1668-1781 (43%)	1670-1950

Table 1. Radiocarbon ages were calibrated to calendar ages by using CALIB Rev 6.0 software (Stuiver and Reimer, 1993) based on Reimer et al. (2009) calibration data set. Some conventional ^{14}C BP dates have multiple intercepts in the calendar year BP curve. Two Sigma calibrated age is provided in ranges with indication of their relative area (in %) under 2σ distribution.

Table 2

Profile ID/ Sample-ID	Lab No.	Depth (m)	K %	U (ppm)	Th (ppm)	Ext.γ (μGy/a)	Cosmic (μGy/a)	Ext. β (μGy/a)	Total dose Rate (μGy/a)	No. of aliquots [a]	De (Gy)[b]	Age (yr)	Age range (years AD)
B1-0													
B1-0/8	BFL-2	1.15	3.90	6.2	52	3901	182	4571	8707±142	18 (36)	8.9±0.9	**1000±100** [c]	**910-1110**
										11 (36)	6.0±0.6	**690±70** [c]	**1250-1390**
B1-0/11	BFL-1	1.75	3.74	7.1	57	4186	169	4692	9106±148	12 (13)	31.5±1.6	***3.5±0.2 ka***	
B1-2													
B1-2/11	BFL-3	1.35	4.07	5.9	63	4404	177	4902	9543±155	7 (13)	4.2±0.3	**440±40**	**1530-1610**
K1													
K1/19	BFL-5	1.6	3.49	5.3	36	2990	172	3815	7017±115	7 (13)	4.9±0.3	**700±40**	**1270-1350**
K1/23	BFL-4	2.65	3.90	4	32	2765	151	3833	6783±113	9 (13)	5.4±0.3	**800±50**	**1160-1260**
K-13													
K13/7	BFL-7	1.5	3.32	7.9	35	3184	174	4001	7405±121	8 (13)	2.5±0.15	**330±20**	**1660-1700**
K13/15	BFL-6	2.6	4.07	5.1	46	3552	152	4408	8159±134	9 (13)	6.9±0.6	**850±70**	**1090-1230**
K13/16	BFL-8	3.2	3.90	5.7	59	4163	142	4671	9033±147	11 (13)	6.6±0.6	**730±70**	**1210-1350**

Table 2. Optically stimulated luminescence dating results from slackwater flood deposits in the Buffels River.

Recycling ratios are within 5% of 1.0. IRSL consist of less than 5% of the OSL signal.
α, β and γ dose rates calculated from the concentrations of the radioisotopes (K, U, Th) and the cosmic dose rates estimated from burial depths.
α contribution is 30-60 μGy/a (not in Table). Water content estimated at 5±2%.
[a]Number of replicated equivalent dose (De) estimates used to calculate the mean. Figures in parentheses indicate total number of measurements made including failed runs.

[b] De: Equivalent dose (Gy).
[c] 23 small aliquots (100-200 grains) were also measured for sample B1-0/8 and their results were combined with the regular measurements. There is a bi-modal distribution of De values which may indicate poorly bleached grains. This is not uncommon in fluvial sediments. Ages are shown for both groups.

Figure 1

Click here to download high resolution image

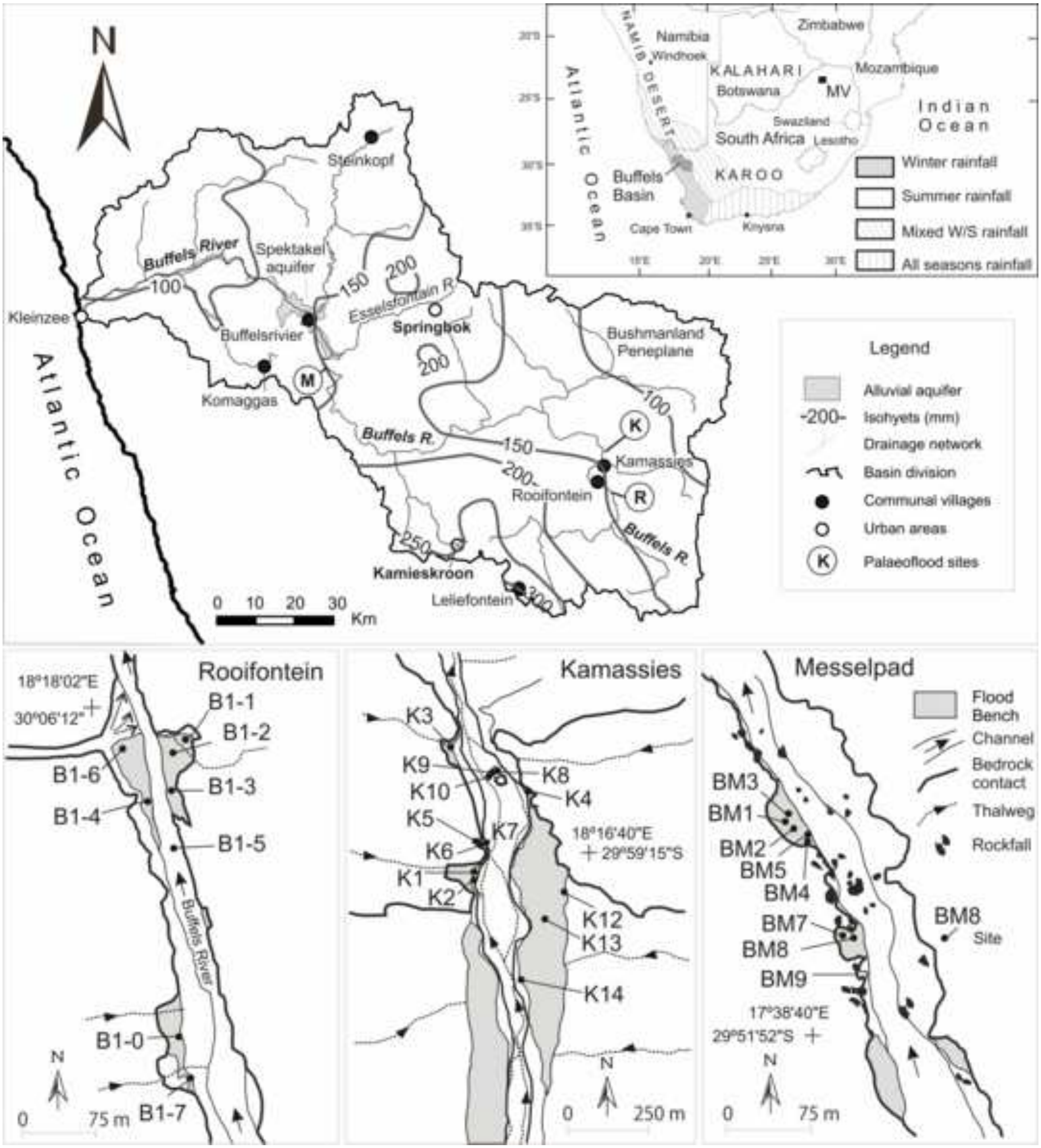

Figure 2

Click here to download Figure: Figure 2.eps

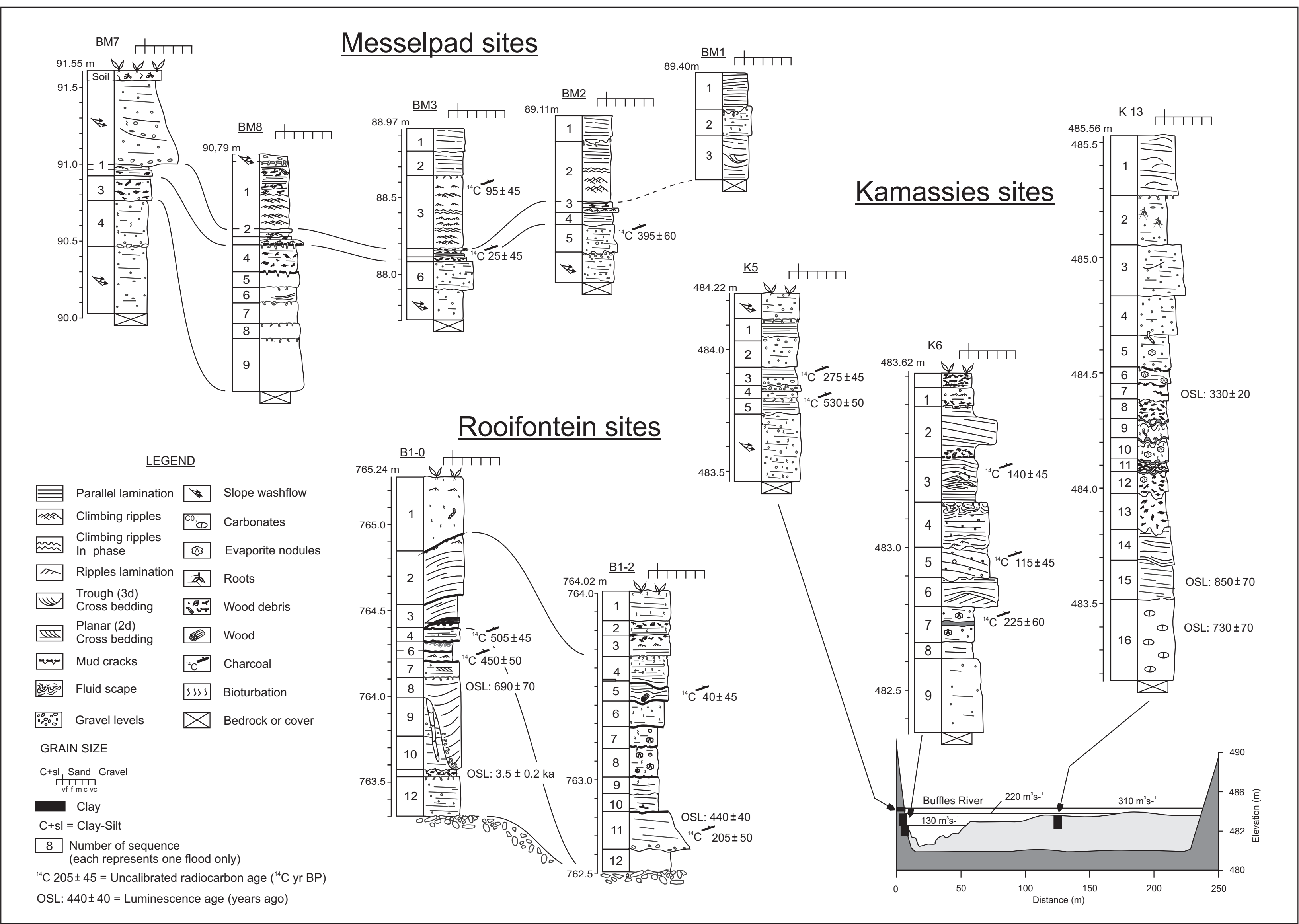

Figure 3
Click here to download high resolution image

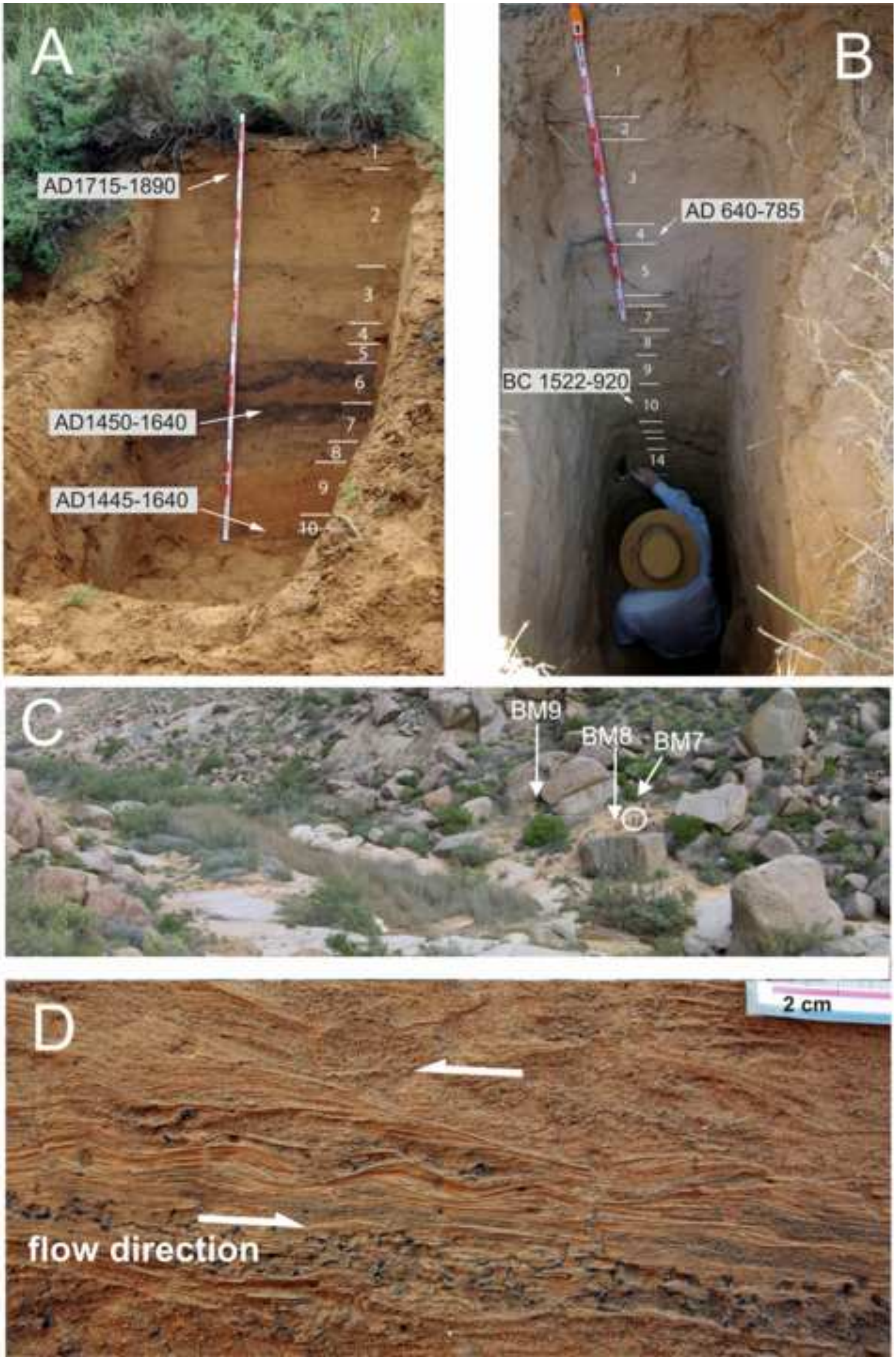

Figure 4
Click here to download Figure: Figure 4.EPS

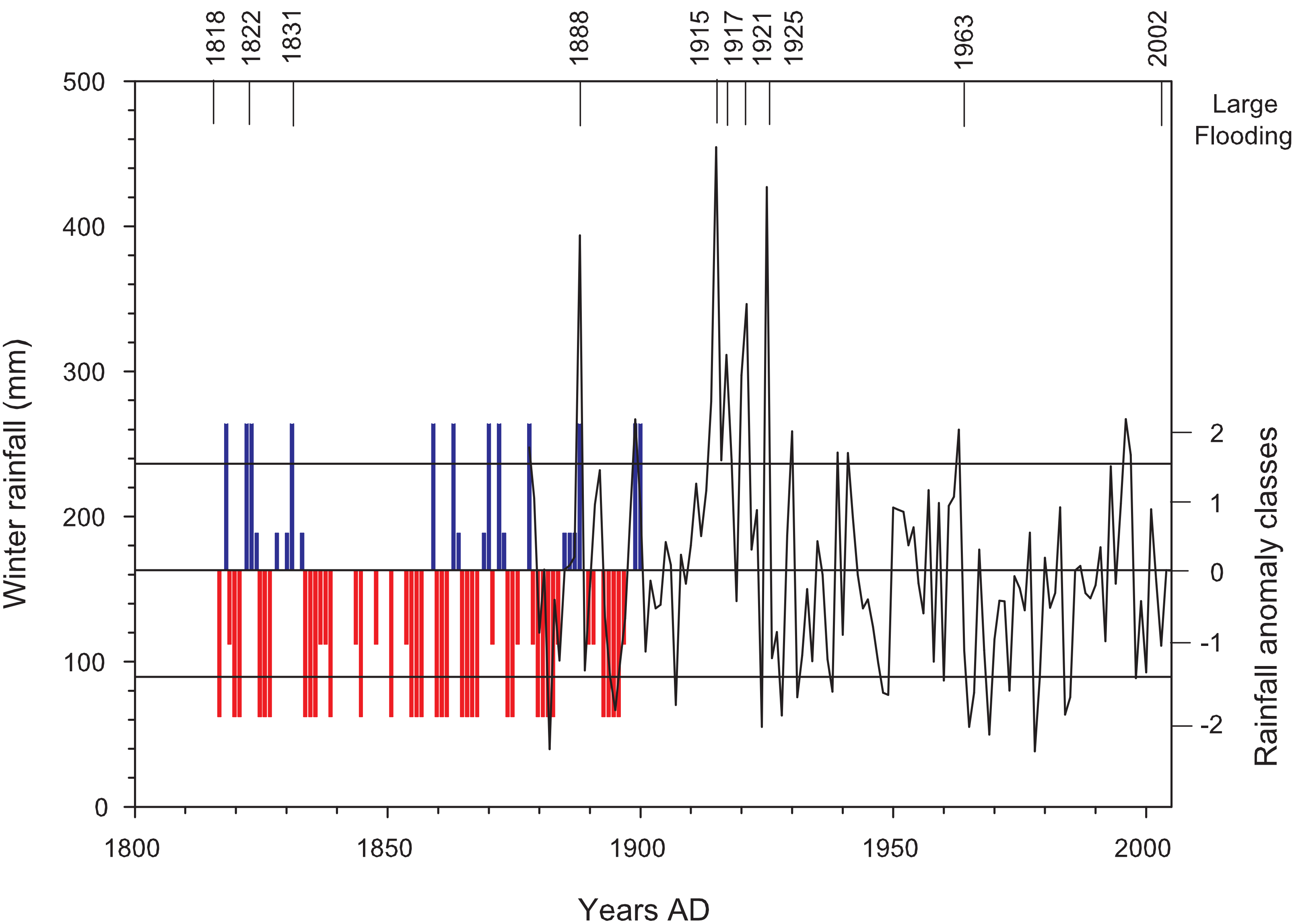

Figure 5

Click here to download Figure: Figure 5.EPS

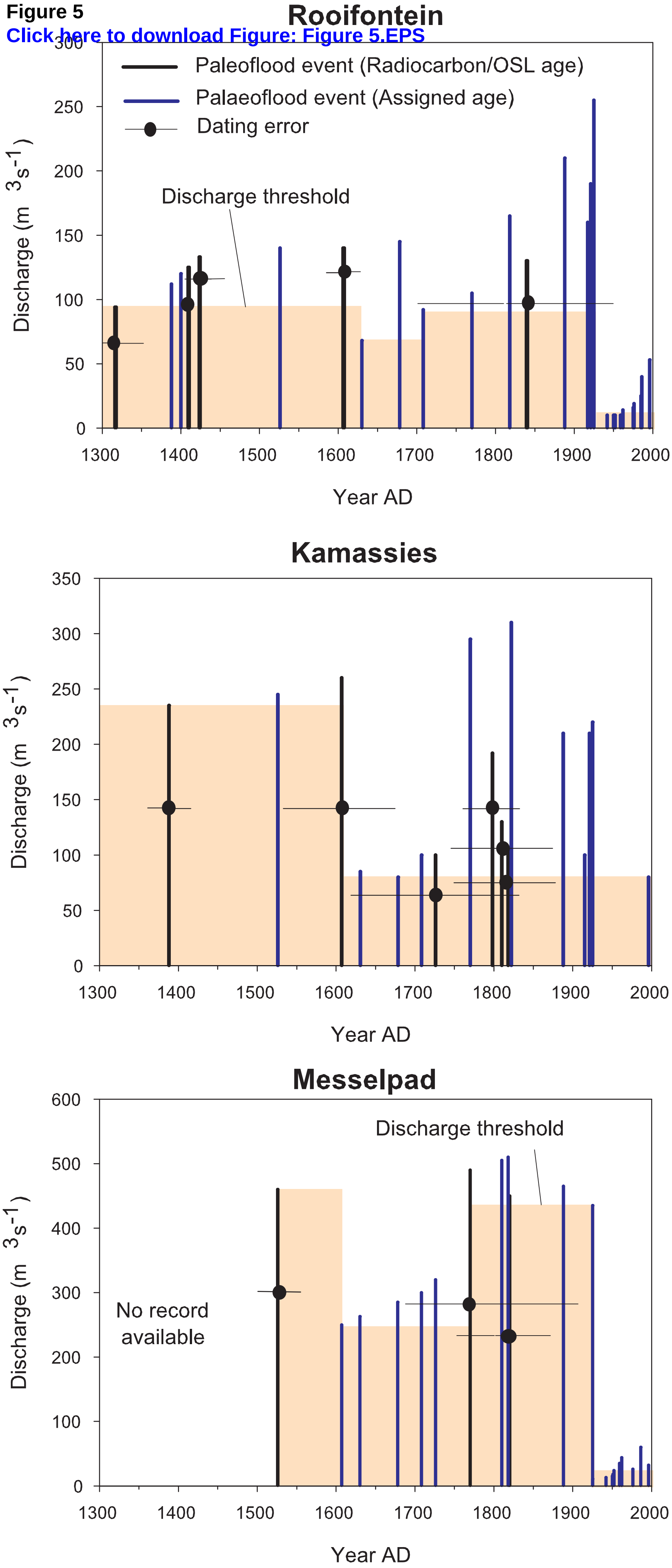

Figure 6
Click here to download Figure: Figure 6.EPS